

Classification of Polarimetric SAR Image based on Improved Fuzzy Clustering

Zheng Cheng^{*}, Ping Han[†], Binbin Han[†] and Jiahui Sun^{*}

^{*}Basic Experiment Center, Civil Aviation University of China, Tianjin, China
E-mail: zcheng_10@163.com, jhsun_yjs@163.com Tel: +86-15202281737

[†]Tianjin Key Laboratory of Advanced Signal and Image Processing, Civil Aviation University of China, Tianjin, China
E-mail: hanpingcauc@163.com, bbhan_11@126.com Tel: +86-22-24092450

Abstract— This paper presents an improved fuzzy clustering approach for Polarimetric SAR image by incorporating neighborhood information. Firstly, polarimetric scattering characteristics of the terrain in PolSAR image are used to generate appropriate initial centers to avoid the issue that FCM is sensitive to random class centers. Then to further enhance the robustness to speckle noise, the conventional robust fuzzy C-mean clustering approach is improved. The work mainly exists in two aspects: (1) The revised Wishart distance is adopted as the data distance measure instead of Euclidean distance to assign a label to each pixel. (2) A weighted fuzzy membership is established by considering local spatial distance and class membership between the central pixel and its neighborhood simultaneously. Finally, the real polarimetric SAR data is utilized for the validation of the proposed unsupervised classification method. Experimental results demonstrate the superiority of the proposed method over the comparisons.

Keywords: Polarimetric SAR; unsupervised classification; fuzzy clustering; neighboring information; revised Wishart distance;

I. INTRODUCTION

Polarimetric synthetic aperture radar (PolSAR) [1] is an advanced remote sensing radar system that can obtain scattering mechanisms of diverse terrains by emitting and receiving different polarized radar waves. It can work all day in any weather condition, and provide more significant information on terrains than single polarization case in various applications, such as target detection, terrain classification, topography extraction. These successful applications of PolSAR rely on image interpretation techniques to a great extent, among which PolSAR image classification is arguably the most important topic and fundamental step to study the enormous amount of PolSAR data.

Many supervised and unsupervised classification approaches [1-6] have been presented in recent years. Supervised algorithms can achieve more precise and reliable results than unsupervised algorithms with a good training data set. However, the performance is restricted to training samples, and the training process requires a lot of time cost and has a lack of automation. Fuzzy C-mean clustering (FCM)

algorithm is a well-known unsupervised classification method which allows each pixel to belong into all clusters with a certain degree of membership, and has been extensively applied in PolSAR image applications. Park [7] proposed an expansion of the hybrid H/α Wishart classifier with the introduction of fuzzy concept in the H/α plane. Zhang [8] proposed an improved fuzzy classification method to constrain speckle noise. Fan [9] adopted the Pauli RGB color features as the input of FCM. Yu [10] proposed a kernel fuzzy C-mean method for image classification. These methods do not either associate polarization parameters with fuzzy theory, or consider the spatially neighboring information between pixels. The performance of these methods is sensitive to the inherent speckle noise.

To improve the classification accuracy and robustness to speckle noise, this paper presents an improved fuzzy clustering approach for polarimetric SAR image by incorporating neighboring information. There are three main contributions in this letter.

1) To overcome the drawback that FCM is sensitive to initial centers, the scattering properties of PolSAR data are combined to partition original image to obtain appropriate initial centers.

2) The revised Wishart distance is adopted as data dissimilarity measure instead of Euclidean distance to obtain better classification results.

3) To promote the robustness to noise, a weighted fuzzy membership is established by considering local spatial distance and class membership differences between the central pixel and its neighborhood simultaneously.

The remainder of this paper is organized as follows. The related work is introduced in Section II. The proposed method is presented in detail in Section III. The experimental results on PolSAR image are delineated in Section IV. Finally, conclusion is given in Section V.

II. RELATED WORK

A. Robust Fuzzy C-mean Clustering Method

Fuzzy clustering, a process of multiple-class pixel assignment, allows each pixel to belong into multiple classes, but with varying membership degree. It is an unsupervised classification approach and assigns a class label to each pixel by the maximum membership degree rule. Let

This work was supported in part by the National Science Foundation of China under Grant 61571442 and Grant 61471365, in part by the National Key Research and Development Program of China under Grant 2016YFB0502405, and in part by the National University's Basic Research Foundation of China under Grant 3122014C004.

$X = \{x_1, x_2, \dots, x_N\}$ be a finite remote sensing data set to represent the whole image, and N is the total number of pixels in the PolSAR image. Assuming that there are c classes, u_{ik} denotes the membership degree of pixel x_i in k th class, $u_{ik} \in [0,1]$ and $U=[u_{ik}]$ is the associated membership matrix. The set of cluster centers is denoted by $V=[v_1, v_2, \dots, v_c]$. Each pixel x_i satisfies the membership constraint $\sum_{k=1}^c u_{ik} = 1$. The robust fuzzy C-mean clustering method (RFCM) [11] divides the whole image into c classes via minimizing the objective function:

$$J(U, V) = \sum_{k=1}^c \sum_{i=1}^N u_{ik}^m \rho(d_{ik}) \quad (1)$$

where m is a weighting exponent controlling the degree of fuzziness and chosen to be 2 for all the runs. $\rho(\cdot)$ denotes Huber function. d_{ik} denotes the Euclidean distance from pixel x_i to the cluster center v_k .

The minimizing process is a constrained optimization problem. To solve it, the Lagrange multiplier technique is introduced with the constraint $\sum_{k=1}^c u_{ik} = 1$, as shown in (2).

$$F = \sum_{k=1}^c \sum_{i=1}^N u_{ik}^m \rho(d_{ik}) + \sum_{i=1}^N \lambda (1 - \sum_{k=1}^c u_{ik}) \quad (2)$$

Taking the derivative with respect to u_{ik} and equating to zero yield

$$\frac{\partial F}{\partial u_{ik}} = m u_{ik}^{m-1} \rho(d_{ik}) - \lambda = 0 \quad (3)$$

according to (3), it is obtained that

$$u_{ik} = \left(\frac{\lambda}{m \rho(d_{ik})} \right)^{\frac{1}{m-1}} \quad (4)$$

substituting the above equation to the constraint condition $\sum_{k=1}^c u_{ik} = 1$, the updating rule of membership u_{ik} is obtained as in (5).

$$u_{ik} = \frac{1}{\sum_{j=1}^c \left(\frac{\rho(d_{ik})}{\rho(d_{ij})} \right)^{\frac{1}{m-1}}} \quad (5)$$

adopting the same approach, the cluster centers v_k can be updated by (6).

$$v_k = \frac{\sum_{i=1}^N u_{ik}^m \omega_{ik}(d_{ik}) x_i}{\sum_{i=1}^N u_{ik}^m \omega_{ik}(d_{ik})} \quad (6)$$

where $\omega_{ik}(d_{ik})$ denotes the Huber weight function, which is capable of reducing the effect of noise. And it is defined by $\omega(x) = \rho'(x)/x$. $\omega_{ik}(d_{ik})$ and Huber function $\rho(d_{ik})$ are both dependent on the distance d_{ik} [12]. In this paper, $\rho(d_{ik})$ is defined by

$$\rho(x) = \begin{cases} 0.5x^2 & |x| \leq 1 \\ |x| - 0.5 & |x| > 1 \end{cases} \quad (7)$$

$\omega_{ik}(d_{ik})$ is defined by

$$\omega(x) = \begin{cases} 1 & |x| \leq 1 \\ 1/|x| & |x| > 1 \end{cases} \quad (8)$$

when $\rho(d_{ik})=d_{ik}$ and $\omega_{ik}(d_{ik})=1$ are both satisfied, the robust fuzzy C-mean method can be considered as conventional FCM. With the introduction of Huber function, RFCM has better performance of resistance to noise and outlier than that of FCM.

B. Dissimilarity Measure Between Pixels

Dissimilarity measure is very significant for unsupervised classification. In classical RFCM, Euclidean distance is adopted as data dissimilarity measure, which is simple and fast, and can work well on noise-free image. However, when it is applied in PolSAR image, the result is unsatisfactory and poor due to the speckle noise caused by the special imaging mechanism of PolSAR. It is known that the PolSAR data follows complex Wishart distribution, which has been extensively used in various PolSAR applications. Hence, this paper adopts the revised Wishart distance [13] as dissimilarity measure, which is derived from complex Wishart distribution. The distance d_{RW} is defined by

$$d_{RW}(\mathbf{T}_i, \mathbf{V}_k) = \ln \frac{|\mathbf{V}_k|}{|\mathbf{T}_i|} + \text{trace}(\mathbf{V}_k^{-1} \mathbf{T}_i) - q \quad (9)$$

where \mathbf{T}_i denotes the coherency matrix of pixel x_i . \mathbf{V}_k is the coherency matrix of k th cluster center, and $\mathbf{V}_k = \sum_{j=1}^{N_k} \mathbf{T}_j / N_k$. N_k is the number of pixels in k th class. $|\cdot|$ denotes the determinant of a matrix. The superscript -1 denotes inverse operator. \ln and trace denote logarithmic operation and trace operation, respectively. q is a constant and chosen to be 3 for the experiment.

To speed up the calculation of distance d_{RW} , inspired by [14], the 3-by-3 coherence matrix \mathbf{T} are transferred into the vector form as

$$f(\mathbf{T}) = [T_{11}, T_{21}, T_{31}, T_{12}, T_{22}, T_{32}, T_{13}, T_{23}, T_{33}]' \quad (10)$$

And let

$$\mathbf{W} = [\omega_1, \omega_2, \dots, \omega_m, \dots, \omega_c]' \quad (11)$$

$$\mathbf{B}_i = [\ln|\mathbf{V}_1|, \ln|\mathbf{V}_2|, \dots, \ln|\mathbf{V}_m|, \dots, \ln|\mathbf{V}_c|]' \quad (12)$$

$$\mathbf{B}_i = [\ln|\mathbf{T}_i| + q, \ln|\mathbf{T}_i| + q, \dots, \ln|\mathbf{T}_i| + q, \dots, \ln|\mathbf{T}_i| + q]' \quad (13)$$

where $\omega_m = f((\mathbf{V}_m^{-1})')$. \mathbf{B}_i denotes a c -by-1 column vector and c is the number of clusters. Thus, the revised Wishart distance (9) can be simplified as follows

$$\mathbf{D} = \mathbf{B}_i - \mathbf{B}_i + \mathbf{W}f(\mathbf{T}) \quad (14)$$

The simplified calculation method improves the computational efficiency tremendously by reducing a large amount of redundant operations in every trace operation and supporting linear calculation method.

III. PROPOSE METHOD

A. Initialization

Fuzzy clustering algorithm has the shortcoming that it is sensitive to the initial centers. Different initial cluster centers may result in different classification results. And appropriate cluster centers can improve the performance of classification and accelerate the convergence speed. To overcome this drawback, polarimetric scattering entropy and Freeman decomposition are combined to segment the original PolSAR image to obtain appropriate cluster centers instead of randomly selected centers. The strategy of classification is as shown in Tab.1. Entropy denotes the polarimetric scattering entropy. P_s , P_d , P_v denote surface scattering power, even scattering power and volume scattering power, respectively. The details are described in [15].

Tab.1 The strategy of selecting initial centers

Entropy	Freeman	Classification results
Entropy<0.5	$P_s > P_d, P_v$	surface scattering
	$P_d > P_s, P_v$	even scattering
	$P_v > P_s, P_d$	volume scattering
0.5<Entropy<0.9	$P_s > P_d > P_v$	surface-even scattering
	$P_s > P_v > P_d$	surface-volume scattering
	$P_d > P_s > P_v$	even-surface scattering
	$P_d > P_v > P_s$	even-volume scattering
	$P_v > P_s > P_d$	volume-surface scattering
Entropy >0.9	$P_v > P_d > P_s$	volume-even scattering
		others

B. A Weighted Membership by Incorporating Neighboring Information

Pixels in an image are highly related to its neighboring pixels, and there is a great possibility that they belong to the same category. To make full use of the neighboring information, this paper modifies the membership u_{ik} by a weighted factor, which considers local spatial distance and class membership between the central pixel and its neighborhood simultaneously. Assuming that the central pixel is denoted by x_i , and the pixels in its neighborhood N_i are denoted by x_r , as shown in Fig.1.

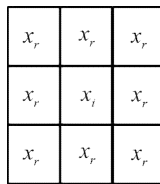


Fig.1 Diagram of a pixel and its neighborhood
The weighted factor is expressed as

$$h_{ik} = \sum_{j \in N_i, i \neq j} \frac{1}{1 + D_{ij}} u_{jk} \quad (15)$$

where u_{jk} denotes the membership of the neighboring pixel x_r in k th class. D_{ij} denotes the spatial distance between the central pixel and its neighboring pixels. $\frac{1}{1 + D_{ij}}$ controls the

contribution of the neighborhood data points to the central data. The closer to the central pixel, the greater contribution to the central pixel. Similar to the membership u_{ik} , h_{ik} reflects the possibility that pixel x_i belongs to the k th class. If most of pixels in a neighborhood N_i belong to the same category, the central pixel x_i is more likely to obtain same category label. Thus, the weighted membership can be expressed as follows.

$$u_{ik}^* = \frac{u_{ik} h_{ik}}{\sum_{j=1}^c u_{ik} h_{jk}} \quad (16)$$

where u_{ik}^* is normalized membership. When the central pixel x_i is a noise point, its membership could be changed by the neighborhood information weighted factor. Thus, the weighted membership can have better performance of robustness and noise insensitiveness. The new centers are updated as

$$v_k = \frac{\sum_{i=1}^N u_{ik}^* \omega_{ik}(d_{ik}) x_i}{\sum_{i=1}^N u_{ik}^* \omega_{ik}(d_{ik})} \quad (17)$$

The flowchart of the proposed method is given in Fig.2, and the detailed classification steps are as follows:

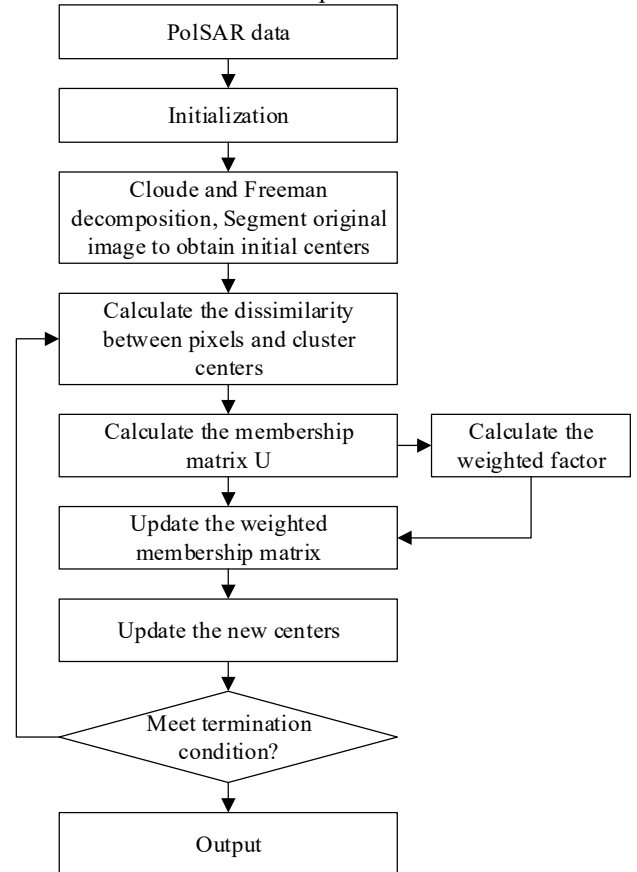


Fig.2 Flowchart of the proposed method

1. Set exponent m , termination ε , maximum iteration number T , the iterative index $t=1$, the window size of neighborhood $W=5$.
2. Apply Cloude decomposition and Freeman decomposition to obtain the polarimetric scattering entropy and power.
3. Segment original image into multiple classes to obtain appropriate initial centers according to the rule in Tab.1.
4. Use (9) and (14) to measure the dissimilarity between pixels and cluster centers.
5. Use (5) to construct the membership matrix $U=[u_{ik}]$.
6. Calculate the weighted factor by (15), and update the weighted membership matrix $U=[u_{ik}^*]$ by (16).
7. Update the new centers by (17).
8. if $\|v_k^{t+1} - v_k^t\| < \varepsilon$ or $t > T$, then stop, else set $t=t+1$ and go to step 4.
9. Assign a category label to each pixel according to the maximum membership rule and output the classification result.

IV. EXPERIMENTAL RESULTS AND ANALYSIS

Two real PolSAR image data set has been used experimentally to validate the performance of the proposed method with which RFCM in [8], KFCM in [10] and H/ α -Wishart in [16] have been compared. The discussion on the classification results in this paper is mainly aimed at Flevoland data. The data of Flevoland area is a subset of an L-Band multilook PolSAR image, which is obtained by the AIRSAR platform in 1989. The color image obtained by Pauli decomposition is shown in Fig.3(a), whose size is 427×299. The ground truth map is shown in Fig.3(b). The scene covers bare soil, potatoes, beet, wheat, peas, lucerne, barley. The classification results with different methods are described in Fig.4. The confusion matrix of the Flevoland area based on the proposed method is shown in Tab.2. And Tab.3 shows the classification accuracy of different methods.

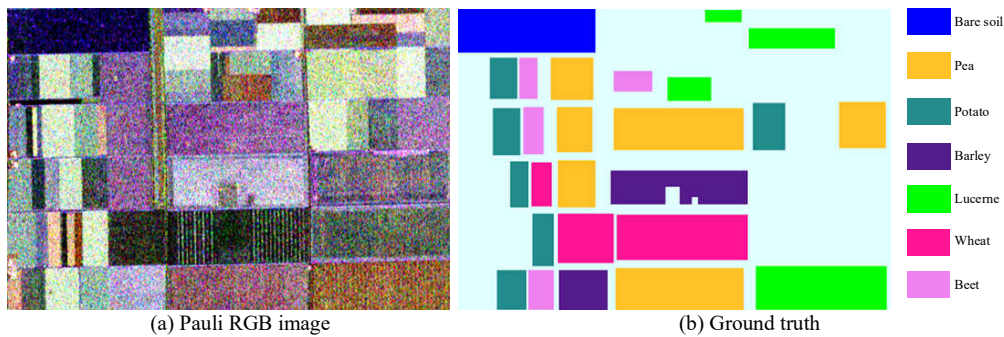


Fig.3 Flevoland area

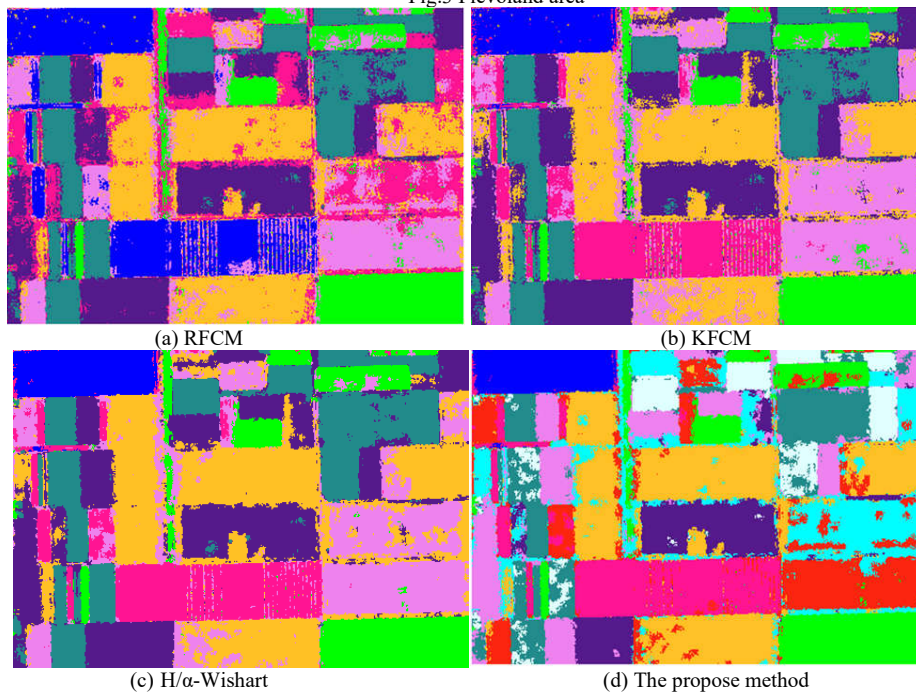


Fig.4 Classification results with different methods

Tab.2 Confusion matrix of the Flevoland area based on the proposed method

Class Region	1	2	3	4	5	6	7	8	9	10
bare soil	96.20	0.26	0.00	0.02	0.00	2.60	0.00	0.00	0.62	0.31
pea	0.00	93.93	0.00	0.06	0.04	0.00	0.00	0.00	3.36	2.61
potato	0.00	0.00	67.94	0.00	0.00	0.00	0.07	31.94	0.00	0.04
barley	0.00	4.57	0.16	91.34	0.31	0.00	0.56	0.76	0.47	1.83
lucerne	0.00	0.00	0.02	0.00	94.46	0.06	0.17	0.00	5.11	0.17
wheat	0.00	0.39	0.00	0.03	0.10	88.13	0.04	0.00	11.26	0.04
beet	0.00	0.00	0.53	0.09	0.00	0.00	99.30	0.00	0.00	0.09

Fig.4(a) shows the classification result of RFCM. From Fig.4(a), we can find that some parts of wheat are recognized as bare soil and some parts of wheat are recognized as others. Beets are almost misclassified into barley class, and we could not find even a pixel of beet is on the corresponding region of ground truth map. The classification accuracy of wheat and beet are 1.31% and 0.00%, respectively. The classification result is the worst and the overall accuracy (OA) of this method is 72.82%. From Fig.4(b), we can find beets are also misclassified into barley class, and the accuracy of beets is zero. However, the classification result of lucerne is better than that obtained by the other methods. And the accuracy is up to 97.21%. OA of the KFCM method is up to 85.25%. From Fig.4(c), we can find that the H/ α -Wishart method can obtain good classification result except the region of beet class. The result of potatoes is the best and the classification accuracy is up to 99.81%. the OA is up to 88.09%. Fig.4(d) shows the classification result of the proposed method. From Fig.4(d), we can find that some parts of potato are misclassified into others, the rate of which is up to 31.94%. Due to considering the local neighbouring information, the proposed method has better robustness to noise and acquires a better classification in the barley region. From Tab.3, we can find that OA of the proposed method is 90.25%, which is higher than the other comparison methods. In a word, the proposed method has a better performance than the other comparisons.

Tab.3 Classification accuracy comparison

	RFCM	KFCM	H/ α -Wishart	the proposed method
bare soil	97.42	94.03	95.88	96.20
peas	90.59	84.79	91.18	93.93
potato	99.22	99.35	99.81	67.94
barley	89.83	89.95	90.57	91.34
lucerne	92.33	97.21	95.99	94.46
wheat	1.31	87.04	91.79	88.13
beet	0.00	0.12	0.00	99.30
Overall Accuracy	72.82	85.25	88.09	90.25

V. CONCLUSION

To improve the robustness to speckle noise and PolSAR image classification accuracy, this paper presents an improved

fuzzy clustering method for PolSAR image classification. Firstly, polarimetric scattering characteristics are used to acquire good initial centers. Then, the membership is weighted by a factor incorporating local spatial distance and class membership between the central pixel and its neighborhood simultaneously. Finally, the revised Wishart distance and modified membership are utilized to classify PolSAR date set into multiple groups. Experimental results show that the performance of the proposed method is better than that of the three comparisons.

REFERENCES

- [1] Song W., Li M., Zhang P., Wu Y., "Fuzziness Modeling of Polarized Scattering Mechanisms and PolSAR Image Classification Using Fuzzy Triplet Discriminative Random Fields," *IEEE Tran. Geosci. Remote Sens.*, pp. 1-14, 2019.
- [2] Nazarinezhad, J. and M. Dehghani, "A contextual-based segmentation of compact PolSAR images using Markov Random Field (MRF) model," *INT. J. Remote Sens.*, vol. 40, pp. 985-1010, 2019.
- [3] Fan J., Zhao J., An W., Hu Y., "Marine Floating Raft Aquaculture Detection of GF-3 PolSAR Images Based on Collective Multikernel Fuzzy Clustering," *IEEE J. Sel. Top. Appl. Earth Observations Remote Sensing*, pp. 1-14, 2019.
- [4] Fan J., Wang X., Wang X., Zhao J., Liu X., "Incremental Wishart Broad Learning System for Fast PolSAR Image Classification," *IEEE Geosci. Remote Sensing Letters*, pp. 1-5, 2019.
- [5] Huang, K., W. Nie and N. Luo, "Fully Polarized SAR imagery Classification Based on Deep Reinforcement Learning Method Using Multiple Polarimetric Features," *IEEE J. Sel. Top. Appl. Earth Observations Remote Sensing*, pp. 1-12, 2019.
- [6] Yang, G., et al., "Unsupervised Change Detection of SAR Images Based on Variational Multivariate Gaussian Mixture Model and Shannon Entropy," *IEEE Geosci. Remote Sensing Letters*, vol. 16 pp. 826-830, 2019.
- [7] Park, S. and W. M. Moon, "Unsupervised Classification of Scattering Mechanisms in Polarimetric SAR Data Using Fuzzy Logic in Entropy and Alpha Plane," *IEEE Tran. Geosci. Remote Sensing*, vol.45, pp. 2652-2664, 2007.
- [8] Tao, Z., S. Jiantao and Y. Ruliang, "Fuzzy classification of polarimetric SAR images," *Systems Engineering and Electronics*, vol. 33, pp. 1036-1039, 2011.
- [9] Fan, J. and J. Wang. "A two-pass unsupervised clustering algorithm for polarimetric SAR image segmentation," *OCEANS, Bergen*, p. 1-5, 2013.

- [10] Yu J., Yan Q., Zhang Z., Ke H., Zhao Z., Wang W.. "Unsupervised classification of polarimetric synthetic aperture radar images using kernel fuzzy C-means clustering," *Int. J. Image Data Fusion*, vol. 3, pp. 319-332, 2011.
- [11] Kersten P. R., Lee J., Ainsworth T.. "Unsupervised classification of polarimetric synthetic aperture Radar images using fuzzy clustering and EM clustering," *IEEE Tran. Geosci. Remote Sensing*, vol. 43, pp.519-527, 2005.
- [12] Frigui H , Krishnapuram R . "A robust competitive clustering algorithm with applications in computer vision," *IEEE Trans. Pattern Analysis and Machine Intelligence*, vol. 21, pp.450-465, 1999.
- [13] Conradsen K , Nielsen A A , Schou J , et al. "A test statistic in the complex Wishart distribution and its application to change detection in polarimetric SAR data," *IEEE Tran. Geosci. Remote Sensing*, vol. 41, pp. 4-19, 2003.
- [14] Jiao L , Liu F . "Wishart Deep Stacking Network for Fast POLSAR Image Classification," *IEEE Trans. Image Processing*, vol. 25, pp.3273-3286, 2016.
- [15] P. Han, Z. Cheng, L. Chang. " Automatic Runway Detection Based On Unsupervised Classification In PolSAR Image," 2016 Integrated Communications Navigation and Surveillance, USA, p. 6E3-1 -6E3-8, 2016.
- [16] Zhu T , Yu J , Li X , et al. Polarimetric synthetic aperture radar image classification using fuzzy logic in the H/ α -Wishart algorithm[J]. *Journal of Applied Remote Sensing*, 2015, 9(1):096098-1-18.